

Surface segregation effects of erbium in GaAs growth and their implications for optical devices containing ErAs nanostructures

Adam M. Crook,^{a)} Hari P. Nair, and Seth R. Bank

The University of Texas at Austin, Microelectronics Research Center, 10100 Burnet Rd. Bldg. 160, Austin, Texas 78758, USA

(Received 13 December 2010; accepted 14 February 2011; published online 23 March 2011)

We report on the integration of semimetallic ErAs nanoparticles with high optical quality GaAs-based semiconductors, grown by molecular beam epitaxy. Secondary ion mass spectrometry and photoluminescence measurements provide evidence of surface segregation and incorporation of erbium into layers grown with the erbium cell hot, despite the closed erbium source shutter. We establish the existence of a critical areal density of the surface erbium layer, below which the formation of ErAs precipitates is suppressed. Based upon these findings, we demonstrate a method for overgrowing ErAs nanoparticles with III-V layers of high optical quality, using subsurface ErAs nanoparticles as a sink to deplete the surface erbium concentration. This approach provides a path toward realizing optical devices based on plasmonic effects in an epitaxially-compatible semimetal/semiconductor system. © 2011 American Institute of Physics. [doi:10.1063/1.3565168]

Metallic structures, with feature sizes small compared to the wavelength of optical radiation, have become extremely useful for photonic and plasmonic devices.^{1,2} The integration of metallic nanoparticles (e.g., silver, gold, copper, etc.) is currently limited to *ex situ* deposition about the device periphery, as most metal systems cannot be epitaxially integrated into semiconductors.³ An alternate class of materials, which is compatible with the growth of photonic devices, is required to reach the full potential of nanostructured metallic features. Heterostructures and nanostructures of rare-earth pnictides (RE-V) and conventional III-V semiconductors have received much attention for their promise of epitaxial integration of metallic structures with semiconductors.⁴⁻⁹ In fact, RE-V nanoparticles have shown plasmonic absorption signatures¹⁰ but have not yet been incorporated into plasmonic devices. While this is a broad class of materials, most research has focused on the (Sc)ErAs/GaAs system, due to the small lattice mismatch and maturity of GaAs growth. Palmström⁴ and co-workers achieved high-quality ErAs films grown on GaAs but the overgrown GaAs suffered from a high density of antiphase domains.¹¹ Limiting the ErAs deposition to uncoalesced islands (self-assembled nanoparticles) and seeding the overgrowth with the exposed GaAs dramatically improved the overgrowth quality.^{7,12} This advance enabled the integration of ErAs nanoparticles into a variety of III-V devices including tunnel junctions,^{5,6} multi-junction solar cells,¹³ terahertz photomixers,⁹ and thermoelectrics.¹⁴ However, these devices are based on non-radiative recombination of carriers or scattering of phonons. As such, the optical quality of the materials grown above the ErAs nanostructures has not been carefully studied. Here, we present a detailed study of the impact of ErAs nanoparticles on subsequently grown III-V emitters and develop a method for obtaining high optical quality layers in close proximity to ErAs nanoparticles. We find the unintentional Er-doping of layers, even with the erbium cell shutter closed, prohibits growth of high optical quality III-V layers while the erbium cell is at an elevated temperature. We identify the importance

of surface segregation in erbium incorporation and nanoparticle formation, and utilize the ErAs nanoparticle layers to deplete this unintentional source of erbium doping. It is of particular interest to grow optically active materials in close proximity to the ErAs nanoparticle layers, to integrate plasmonic functionality into semiconductor photonic devices.

Samples were grown by solid-source molecular beam epitaxy in a Varian Gen II system equipped with Ga, In, Al, and Er effusion cells, as well as a valved As cracker. The optical quality of the III-V layers was investigated with room temperature photoluminescence (PL). The samples, shown schematically in the inset of Fig. 1, consisted of an In_{0.15}Ga_{0.85}As quantum well (QW) embedded in a 200 nm GaAs absorbing region, surrounded on either side by 5 nm AlAs carrier blocking layers. The QW was intentionally brought in close proximity (<25 nm) to the underlying ErAs nanostructures, providing maximum sensitivity to any issues associated with the III-V overgrowth of ErAs. The AlAs carrier blocking layers prevent photogenerated carriers

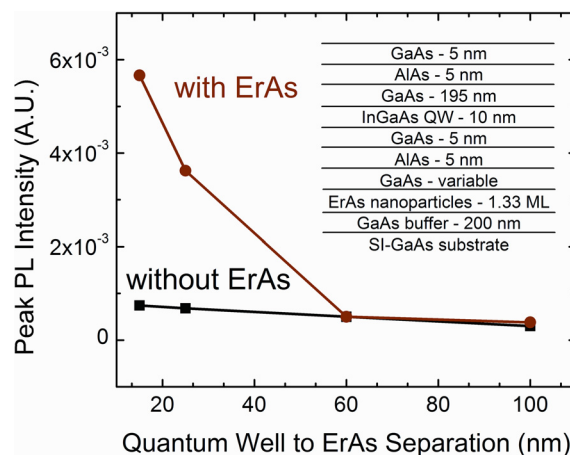


FIG. 1. (Color online) Peak PL intensity for nominally identical PL structures, shown schematically in the inset, grown with varying proximity to a layer of ErAs nanoparticles. A control sample was grown without an ErAs nanoparticle layer for each thickness. The erbium cell temperature was maintained at the growth temperature throughout the growth of each sample.

^{a)}Electronic mail: acrook@mail.utexas.edu.

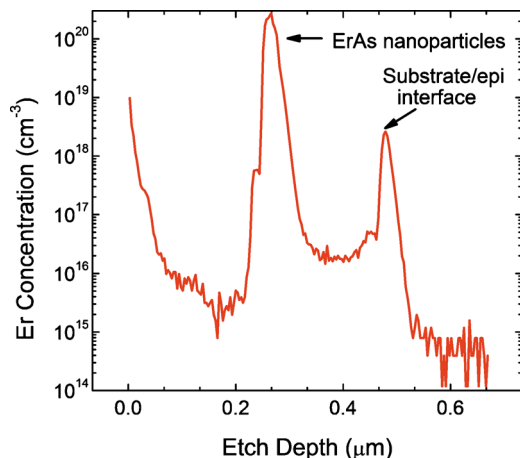


FIG. 2. (Color online) Erbium depth profile measured by SIMS, for the PL sample grown 5 nm from an ErAs nanoparticle layer. Note that (i) there is an accumulation of erbium during thermal removal of native oxide at substrate/epi interface and (ii) that the parasitic erbium incorporation decreased by $\sim 10\times$ immediately following the ErAs nanoparticle layer.

from recombining at the sample surface or in the underlying epitaxial layers, providing maximum sensitivity to nonradiative recombination in the PL structure. The total absorbing thickness (i.e., the spacing between the AlAs layers) was held constant, facilitating comparison between structures as the InGaAs QW was brought progressively closer to the ErAs nanoparticles. Growth conditions, reported elsewhere,⁶ were optimized for tunnel junction resistivity. A set of PL structures were grown with the QW separated by 15, 25, 60, and 100 nm from the underlying ErAs nanoparticle layer, each with a nominally identical control sample without an ErAs layer.

Figure 1 plots the peak PL intensity versus the separation between the InGaAs QW and the ErAs nanoparticles. The peak PL intensity was normalized to a standard PL structure that was grown with the erbium shutter closed and the cell at idle temperature (500 °C). The PL intensity was severely degraded for all samples grown with the erbium cell hot. Nominally identical samples containing a layer of ErAs nanoparticles below the QW exhibited higher PL intensity than the control samples. In fact, PL structures grown in successively closer proximity to the ErAs nanoparticle layer exhibited progressively higher PL intensity.

The degradation of samples grown without ErAs nanoparticles but grown with the erbium cell hot, warranted further investigation. Secondary ion mass spectrometry (SIMS) measurements of Er, Ga, Al, In, and As concentrations, as well as other possible contaminants (O, C, Ta, Pd, Pr, Pb, W, Cr, Fe) were conducted on the PL structure with the ErAs nanoparticle layer 15 nm from the InGaAs QW. The erbium depth profile is shown in Fig. 2. Parasitic erbium incorporation into layers grown with the shutter closed but the erbium cell hot was clearly observed. The erbium incorporation prior to the growth of the ErAs-nanoparticle-layer was $\sim 10\times$ higher than the concentration observed in the early stages of ErAs overgrowth. In the subsequent overgrowth, the erbium concentration increased until a large surface concentration was observed. Gupta *et al.*⁸ have reported reduced lifetimes for Er-doped GaAs. Ancillary time-resolved PL measurements¹⁵ indicated $\sim 10\times$ longer PL lifetime for samples grown after an ErAs nanoparticle layer. This is con-

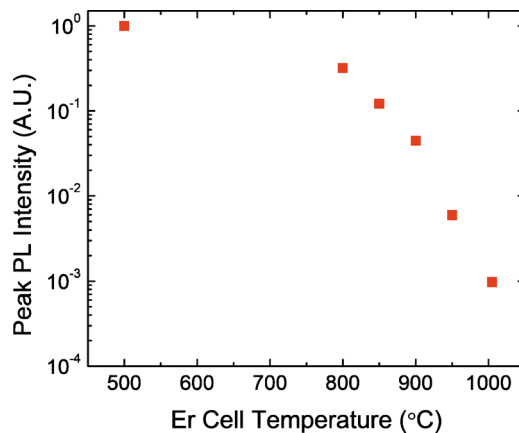


FIG. 3. (Color online) Peak PL intensity for nominally identical PL structures, grown with varying erbium cell temperature. PL intensity degraded in proportion to the erbium flux, over a temperature range between 800 and 1005 °C.

sistent, both qualitatively and quantitatively, with erbium incorporation as the root cause of the reduced luminescence efficiency.

The PL and SIMS observations can be understood with the surface segregation model developed for Er-doping of Si.¹⁶ A parasitic erbium flux is incident on the surface despite the shutter being closed. Erbium segregates to the surface during GaAs growth, causing parasitic erbium incorporation into the GaAs epitaxial layers. The incorporation is kinetically limited by the surface concentration.¹⁷ A steady-state surface concentration is reached when the erbium incorporation into the epitaxial layer equals the parasitic erbium flux. The ErAs nanoparticle layer acts as an alternative incorporation mechanism for the surface erbium layer. In other words, the ErAs nanoparticles act as a sink for erbium, depleting the surface concentration. As will be shown subsequently, as the growth surface moves away from the nanoparticle layer, the erbium diffusion to the ErAs nanoparticles is inhibited, leading to an increase in the erbium surface concentration. Finally, the depleted surface concentration in close proximity to the nanoparticle layer resulted in reduced erbium incorporation until the parasitic erbium flux replenished the surface concentration up to its steady-state value. This growth mode agrees well with the embedded growth mode for ErAs presented by Schultz *et al.*,¹⁸ provided that an ErAs nanoparticle layer is formed at the surface. This model is also consistent with studies of Er-doping of GaAs,¹² in the absence of an underlying ErAs nanoparticle layer.

It is clear that to achieve high optical quality material in close proximity to ErAs nanoparticles, care must be taken to mitigate parasitic erbium incorporation. In particular, the parasitic erbium flux, due to the erbium effusion furnace, must be negligible, and the sample surface must be depleted of erbium prior to growing optically active layers. To this end, ErAs-free PL structures were grown with varying erbium cell temperature to determine the maximum erbium cell temperature that permits high optical quality III-V overgrown layers. Figure 3 plots the peak PL intensity with erbium cell temperature. The observed PL degradation was proportional to the erbium flux. In fact, samples grown with the erbium cell cooled to the idle temperature of 500 °C displayed $\sim 1000\times$ higher intensity than those grown with the erbium cell held at the temperature for ErAs growth,

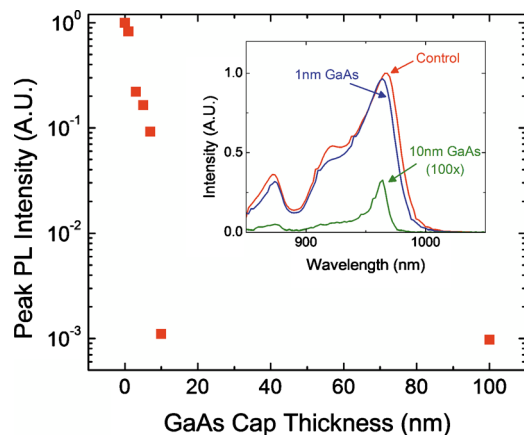


FIG. 4. (Color online) Peak PL intensity for samples grown with varying GaAs spacer thickness between the ErAs nanoparticle layers and the location of the growth interruption. The inset shows the PL spectra for the control, 1 and 10 nm spacer thicknesses. The sample grown with a 1 nm GaAs spacer thickness exhibited PL intensity comparable to samples grown with erbium cell held at idle temperature throughout growth. The sample grown with 10 nm GaAs spacer is scaled by 100 \times and exhibit severely degraded PL intensity.

~ 1000 °C. This finding is in good agreement with the observed degradation in carrier lifetime for erbium-doped GaAs.⁸

To investigate the integration of ErAs nanoparticles with optical quality material, after growth of the ErAs nanoparticle layer, growth was interrupted while the erbium cell was cooled to 500 °C to mitigate the PL degradation associated with parasitic erbium incorporation. During this growth interruption, the parasitic erbium flux must be prevented from accumulating on the surface, to eliminate subsequent incorporation into the optically active regions. Reduced erbium incorporation was observed in the layers grown immediately after the ErAs nanoparticle layer (Fig. 2). This suggests that, after a nanoparticles nucleate, surface erbium preferentially incorporates at these nanoparticles. Therefore, an ErAs nanoparticle layer could be employed to deplete the surface of erbium, during this growth interruption.

To test this hypothesis, a set of samples were grown with a 1.33 ML ErAs nanoparticle layer, followed by a GaAs spacer layer of variable thickness (1, 3, 5, 7, 10, and 100 nm), prior to a growth interruption in which the erbium cell was cooled. During the growth interruption, the substrate temperature was heated to 600 °C, well above the deoxidation temperature of GaAs, to simultaneously enhance erbium diffusion and mitigate unintentional oxygen incorporation. After the erbium cell cooled to 500 °C, the substrate temperature was returned to 530 °C and the remaining PL structure was grown. Figure 4 plots the peak PL intensity versus GaAs spacer thickness. It is clear that the sample with 1 nm GaAs spacer shows comparable optical quality to the control sample grown continuously at a substrate temperature 530 °C with the erbium cell at 500 °C. However, the samples with thicker GaAs spacers showed rapidly decreasing PL intensity with increasing spacer thickness. The comparable luminescence intensity of the samples with 10 and 100 nm GaAs spacers implies that the spacers prevented the parasitic erbium flux from incorporating into the nanoparticles via diffusion. The parasitic erbium accumulated at the

surface during the growth interruption and was subsequently incorporated into the PL structure. Therefore, we conclude that the growth interruption, not the GaAs spacer thickness, is responsible for the PL degradation. These results demonstrate the importance of controlling the surface segregation of erbium in growing high quality semimetal/semiconductor heterostructures.

The optical quality of ErAs nanoparticle overgrowth was investigated. We proposed a model for the incorporation of erbium, in which erbium segregates to the surface until a critical areal density is reached, beyond which surface erbium efficiently incorporates as ErAs nanoparticles. We employed this model to develop a method for depleting the surface of erbium after nanoparticle growth, enabling the overgrowth of ErAs nanostructures with III-V light emitters of comparable optical quality to their Er-free counterparts. These findings provide a pathway toward the active plasmonic devices operating in the near-infrared.

The authors would like to acknowledge Professor Jelana Vuckovic for supporting time resolved PL measurements and Professor Ed Yu for many useful discussions. This work was supported by the Army Research Office (Grant No. W911NF-07-1-0528), monitored by Dr. Mike Gerhold, and the Air Force Office of Scientific Research through the Young Investigator Program (Grant No. FA9550-10-1-0182), monitored by Dr. Kitt Reinhardt.

¹W. L. Barnes, A. Dereux, and T. W. Ebbesen, *Nature (London)* **424**, 824 (2003).

²S. Nie and S. R. Emory, *Science* **275**, 1102 (1997).

³C. J. Palmstrom, *Annu. Rev. Mater. Sci.* **25**, 389 (1995).

⁴C. J. Palmström, N. Tabatabaie, and J. S. J. Allen, *Appl. Phys. Lett.* **53**, 2608 (1988).

⁵P. Pohl, F. H. Renner, M. Eckardt, A. Schwanhauser, A. Friedrich, O. Yuksekdag, S. Malzer, G. H. Dohler, P. Kiesel, D. Driscoll, M. Hanson, and A. C. Gossard, *Appl. Phys. Lett.* **83**, 4035 (2003).

⁶H. P. Nair, A. M. Crook, and S. R. Bank, *Appl. Phys. Lett.* **96**, 222104 (2010).

⁷C. Kadow, S. B. Fleischer, J. P. Ibbetson, J. E. Bowers, A. C. Gossard, J. W. Dong, and C. J. Palmström, *Appl. Phys. Lett.* **75**, 3548 (1999).

⁸S. Gupta, S. Sethi, and P. K. Bhattacharya, *Appl. Phys. Lett.* **62**, 1128 (1993).

⁹J. E. Bjarnason, T. L. J. Chan, A. W. M. Lee, E. R. Brown, D. C. Driscoll, M. Hanson, A. C. Gossard, and R. E. Muller, *Appl. Phys. Lett.* **85**, 3983 (2004).

¹⁰M. P. Hanson, A. C. Gossard, and E. R. Brown, *J. Appl. Phys.* **102**, 043112 (2007).

¹¹C. J. Palmström, K. C. Garrison, S. Mounier, T. Sands, C. L. Schwartz, N. Tabatabaie, S. J. Allen, Jr., H. L. Gilchrist, and P. F. Miceli, *J. Vac. Sci. Technol. B* **7**, 747 (1989).

¹²K. E. Singer, P. Rutter, A. R. Peaker, and A. C. Wright, *Appl. Phys. Lett.* **64**, 707 (1994).

¹³J. M. O. Zide, A. Kleiman-Shwarscstein, N. C. Strandwitz, J. D. Zimmerman, T. Steenblock-Smith, A. C. Gossard, A. Forman, A. Ivanovskaya, and G. D. Stucky, *Appl. Phys. Lett.* **88**, 162103 (2006).

¹⁴W. Kim, S. L. Singer, A. Majumdar, D. Vashae, Z. Bian, A. Shakouri, G. Zeng, J. E. Bowers, J. M. O. Zide, and A. C. Gossard, *Appl. Phys. Lett.* **88**, 242107 (2006).

¹⁵Y. Gong, A. M. Crook, H. P. Nair, S. R. Bank, and J. Vuckovic (unpublished).

¹⁶R. Serna, M. Lohmeier, P. M. Zagwijn, E. Vlieg, and A. Polman, *Appl. Phys. Lett.* **66**, 1385 (1995).

¹⁷J. M. Moison, C. Guille, F. Houzay, F. Barthe, and M. Van Rompay, *Phys. Rev. B* **40**, 6149 (1989).

¹⁸B. D. Schultz and C. J. Palmström, *Phys. Rev. B* **73**, 241407 (2006).